Journal Name

ARTICLE

Diastereomeric Cyclopentane-Based Maltosides (CPMs) as Tools for Membrane Protein Study

Received 00th January 20xx,
Accepted 00th January 20xx

DOI: 10.1039/x0xx00000x

www.rsc.org/

Manabendra Das,[a,b] Florian Mahler,[b] Parameswaran Hariharan,[c] Haoqing Wang,[d] Yang Du,[d] Jonas S. Mortensen,[e] Eugenio Pérez Patallo,[b] Lubna Ghani,[a] David Glück,[b] Bernadette Byrne,[f] Claus J. Loland,[e] Lan Guan,[c] Brian K. Kobilka,[d] Sandro Keller,[b] and Pil Seok Chae*[a]

Amphiphilic agents, called detergents, are invaluable tools for studying membrane proteins. However, membrane proteins encapsulated by conventional head-to-tail detergents tend to denature or aggregate, necessitating the development of structurally distinct molecules with improved efficacy. Here, a novel class of diastereomeric detergents with a cyclopentane core unit, designated cyclopentane-based maltosides (CPMs), were prepared and evaluated for their ability to solubilize and stabilize several model membrane proteins. A couple of CPMs displayed enhanced behaviors compared to the benchmark conventional detergent, *n*-dodecyl-β-D-maltoside (DDM) for all the tested membrane proteins including two G protein-coupled receptors (GPCRs). Furthermore, CPM-*C*12 was notable for its ability to confer enhanced membrane protein stability compared to the previously described conformationally-rigid NBMs (*JACS*, **2017**, *139*, 3072) and LMNG. The effect of the individual CPMs on protein stability varied depending on both the detergent configuration (*cis*/*trans*) and alkyl chain length, allowing us draw conclusions on the detergent structure-property-efficacy relationship. Thus, this study not only provides novel detergent tools useful for membrane protein research, but also reports on sturctural features of the detergents critical for detergent efficacy for protein stabilization.

Introduction

Integral membrane proteins are essential for cell functions such as inter- or intra-cellular material transfer, signal transduction, photosynthetic electron transport, protein trafficking, cell adhesion and comprise more than 50% of human drug targets.[1] Structural and functional information of membrane proteins is essential for fundamental understanding of their mechanism of action as well as for rational design of new drug molecules. Unfortunately, these bio-macromolecules represent ~2-3% of 3D-resolved protein structures,[2] even with the recent advances in cryo-electron microscopy and the substantial successes achieved with X-ray crystallography.[3] Membrane protein extraction, purification and structural investigation are often challenging mainly because of the low natural abundance of these molecules and their tendency to denature or aggregate once extracted from native membranes into aqueous buffer. A key prerequisite for isolation and structural studies of membrane proteins is that they must be maintained in a soluble and stable state in buffer solution by an amphiphilic additive that shields the large hydrophobic protein surfaces from polar aqueous environments. Conventional detergents with a polar head and a hydrophobic tail group such as *n*-dodecyl-β-D-maltoside (DDM), *n*-octyl-β-D-glucoside (OG), and lauryldimethylamine-*N*-oxide (LDAO) are widely used to extract membrane proteins from native lipid-bilayers and to maintain the native states of the proteins in solution.[4,5] However, in addition to being more dynamic than lipid assemblies, detergent micelles tend to expose hydrophobic regions of membrane proteins to buffer solution,[6,7] resulting in irreversible nonspecific aggregation. Thus, it is of great importance to develop novel agents or membrane-mimetic systems displaying favorable behaviors for membrane protein solubilization and stabilization.[8]

Notable examples of several large membrane-mimetic systems are nanodiscs (NDs),[9] amphiphilic polymers [styrene-maleic acid (SMA)[10a] copolymer, diisobutylene-maleic acid (DIBMA)[10b] copolymer, amphipols (APols)],[11] and peptide detergents [β-peptides (BPs),[12] lipopeptide detergents (LPDs),[13a] and Salipro[13b]]. These agents have been shown to maintain several membrane proteins in native-like conformations, but proved to be inefficient at protein extraction and tend to form large protein-detergent complexes (PDCs). More importantly, with few exceptions (e.g. SMA),[10a] they

[a] Dr. M. Das, L. Ghani, Prof. P. S. Chae
Department of Bionanotechnology, Hanyang University, Ansan, 426-791 (Korea)
E-mail: pchae@hanyang.ac.kr
[b] F. Mahler, E. P. Patallo, D. Glück, Prof. S. Keller, Molecular Biophysics, Technische Universität Kaiserslautern, Erwin-Schrödinger -Str. 13, 67663, Kaiserslautern, Germany Email: sandro.keller@biologie.uni-kl.de
[c] Dr. P. Hariharan, Prof. L. Guan
Department of Cell Physiology and Molecular Biophysics, Center for Membrane Protein Research, School of Medicine, Texas Tech University Health Sciences Center, Lubbock, TX 79430 (USA). E-mail: lan.guan@ttuhsc.edu
[d] Dr. H. Wang, Dr. Y. Du, Prof. B. K. Kobilka
Molecular and Cellular Physiology, Stanford, CA 94305 (USA)
E-mail: kobilka@stanford.edu
[e] Dr. J. S. Mortensen, Prof. C. J. Loland
Department of Neuroscience and Pharmacology, University of Copenhagen, DK, 2200 Copenhagen (Denmark) E-mail: cllo@sund.ku.dk
[f] Prof. B. Byrne,
Department of Life Sciences, Imperial College London, London, SW7 2AZ (UK),
E-mail: b.byrne@imperial.ac.uk
[g] † Supporting information for this article is given via a link at the end of the document.See DOI: 10.1039/x0xx00000x

are not able ??to produce protein crystals with high quality. As an alternative strategy, several small amphiphilic agents have been developed as exemplified by neopentyl glycol (NG)-based amphiphiles (MNGs/GNGs/NDTs),[14] mannitol-based amphiphiles (MNAs),[15] tripod amphiphiles (TPAs),[16] calix[4]arene-based amphiphiles (C4Cs),[17] tandem malonate-based glucosides (TMGs),[18] penta-saccharide amphiphiles (PSEs),[19] butane-tetraol-based maltosides (BTMs),[20] glycosyl-substituted dicarboxylate detergents (DCODs),[21] dendronic group-containing trimaltosides (DTMs),[22] and 1,3,5-triazine-cored maltosides (TEMs).[23] GNG-3 and MNG-3 have contributed to the determination of more than 40 membrane protein crystal structures including a sodium-pumping pyrophosphatase, human aquaporin 2 (AQP2), and acetylcholine and opioid G-protein coupled receptors (GPCRs) in the past ten years.[24] Departing from the canonical 'polar head and nonpolar tail' design of conventional detergents, facial amphiphiles (FAs) represent a highly innovative approach for studying membrane proteins and some of these amphiphiles (e.g., FA-5 and FA-7) were utilized for 3D crystal structure determinations of the ATP-binding cassette transporter (MsbA) and the GPCR-like bacteriorhodopsin.[25] Recently we developed norbornane (NB)-based maltosides (NBMs)[26] with two flexible alkyl arms and two maltoside head groups connected by a conformationally locked norbornane linker. Of these agents, X-NBM-C11 showed remarkable stabilization behavior with several model membrane proteins including human β_2 adrenergic receptor (β_2AR). Despite the favorable effects on protein stability, this NBM tends to form larger micelles (hydrodynamic radius (R_h) = 17.3 nm), which is potentially an unfavorable aspect for protein crystallization and NMR-based structural study. In addition, the NB linker used to build the NBMs could be too rigid to maximize detergent efficacy for protein stabilization. Herein, we made our efforts to address these issues by converting the linker from the rigid NB (NBMs) to a more flexible cyclopentane (CP) unit (CPMs) (Fig. 1). This monocyclic linker provides conformational flexibility relative to the bicyclic NB linker, along with a unique degree of preorganization of both hydrophilic and lipophilic moieties. When the new detergents were evaluated with several model membrane proteins including two GPCRs, we found that CPM-*C*12 was significantly better than DDM and X/D-NBM-C11 at stabilizing the membrane proteins tested here.

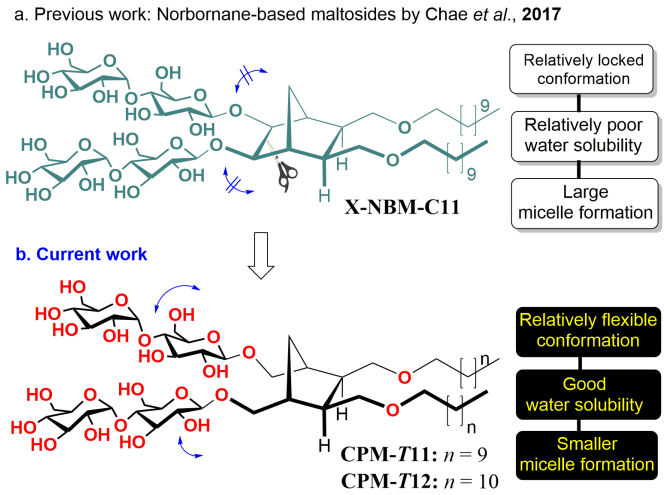

Fig. 1 Background for this study. The chemical structures of (a) previously reported X-NBM-C11 detergent with conformationally restricted maltoside head groups and (b) new cyclopentane-based maltoside-*trans* detergents (CPM-*T*s) with the more conformationally flexible head groups. The CPM-*T*s were created by disconnecting a C-C bond from the norbornane scaffold. The relative conformational flexibility of the head groups is shown by the blue arrows. Unlike X-NBM-C11, these new detergents gave increased water-solubility and formed smaller micelles.

Results and discussion

Detergent structures and physical characterizations

The CPMs feature two alkyl chains and two dimaltosides as the hydrophobic and hydrophilic groups, respectively, connected via a monocyclic CP ring (Fig. 2). Depending on the relative orientation of the alkyl chains with respect to the head groups (*cis*/*trans*), these agents can be categorized into two sets. The two alkyl chains were connected to the C2 and C3 positions of the CP linker in a *cis* configuration (2*R*,3*S*) with respect to the head groups for CPM-*C*s while a *trans* configuration was used for this connection of the alkyl chains in the case of CPM-*T*s (Fig. 2). As a result, the CPM-*C*s and CPM-*T*s are CP variants of X-NBMs and D-NBMs, respectively. Due to the torsional and angle strains of the central CP ring, the CPM-*C*s and CPM-*T*s are likely to preferentially adopt energy-minimized puckered conformations, half chair (***C*₂**) and envelope (***C*ₛ**), respectively (Fig. 2 & S1[†]). This is in contrast to the conformationally-locked NB linker in the NBMs. The configuration (*cis*/*trans*) and conformational variations (half chair (***C*₂**)/envelope (***C*ₛ**)) between the CPM-*C*s and CPM-*T*s could affect amphiphile efficacy for membrane protein stabilization in spite of their identical chemical compositions (*i.e.* identical polar and nonpolar segments). As hydrophile-lipophile balance (HLB) is important in determining detergent property,[27] we prepared detergent variants with two alkyl chain lengths (C11 and C12) for both sets of CPMs, used for detergent designation. Density functional theory (DFT) calculations at a B3LYP/6-31G* level was supportive for a half chair/twist conformation of the CP ring for CPM-*C*11 with a hydrophobic length of 15.2 Å, while its *trans* isomer (CPM-*T*11) was calculated to give an envelope conformation of the CP ring, with the hydrophobic length of 15.1 Å (Fig. S1). Thus, the two different conformations (half chair (**C₂**)/envelope (**Cₛ**)) along with alkyl chain length variations (C11/C12) serve as a way to change or fine-tune the detergent hydrophobic length. This is important as detergent hydrophobic length needs to be compatible with the hydrophobic dimensions of membrane protein for optimal protein stability in solution.

Journal Name

ARTICLE

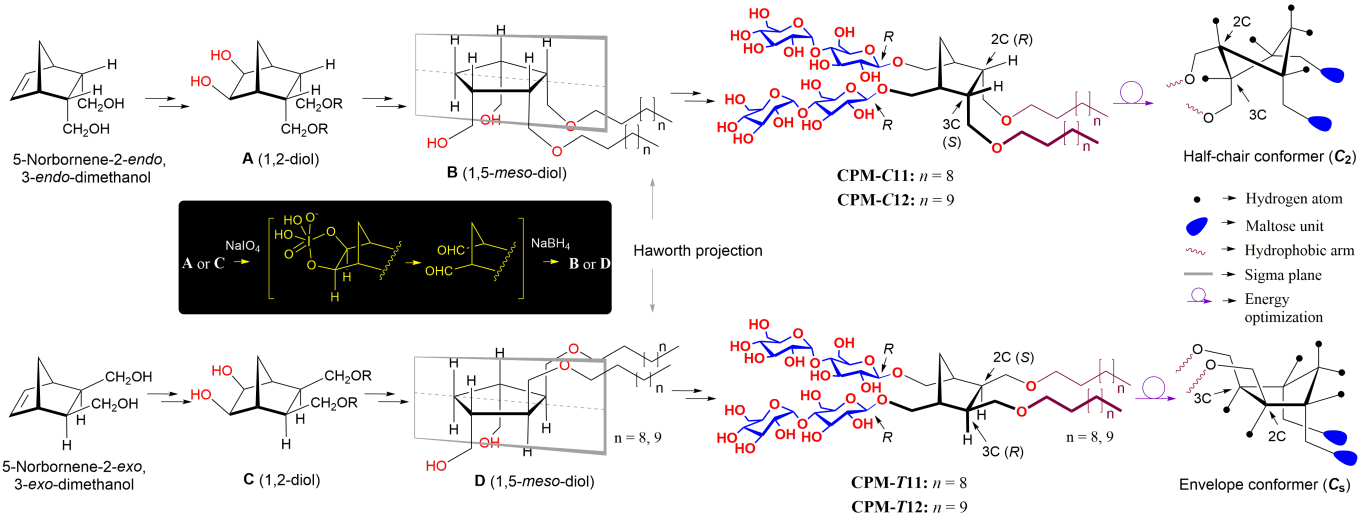

Fig. 2 (a) Chemical structures of novel cyclopentane-based maltosides (CPMs) (middle-right) and their energy-optimized puckered conformers (far right). The CPM-*C*s were derived from 5-norbornene-2-*endo*,3-*endo*-dimethanol, while CPM-*T*s were derived from isomeric 2-*exo*,3-*exo*-dimethanol (far left). *Syn*-dihydroxylation using OsO_4-NMO was used for 1,2-diol generation (**A**/**C**, left). The inset within rectangle represents periodate oxidative cleavage of 1,2-diols (**A** and **C**), followed by $NaBH_4$ reduction to afford 1,5-*meso*-diol derivatives (**B** and **D**). **B** and **D** are *meso* compounds due to the presence of a symmetry plane which perpendicularly bisects the central cyclopentane (CP) ring of the molecule (indicated by gray line in the Haworth projection). The CPM-*C*/*T*samphiphiles commonly contain a dimaltoside head group connected to the two alkyl chains using a cyclopentane linker (middle right). *R* or *S* designation was used to specify the stereochemistry of the two chiral carbons (C2 and C3). Half chair ($\mathbf{C_2}$) and envelope ($\mathbf{C_s}$) are two energy-minimized CP conformations of CPM-*C*s and CPM-*T*s, respectively, optimized by DFT calculations at the energy level of B3LYP/6-31G*)(far right).

The individual hydrophobic groups of the CPM-*C*s/*T*s are optically inactive *meso* compounds due to the presence of an internal symmetry plane dissecting the CP linker (compounds **B** and **D** in Fig. 2). Since these 1,5-*meso*-diols (**B** and **D**) are non-superimposable stereoisomers, they are diastereomers to each other. The CPM-*C*s/*T*s are also diastereomers of each other, but are optically active because of the lack of an internal symmetry plane. The new agents were prepared according to a protocol comprising five high-yielding synthetic steps: (1) dialkylation, (2) alkene *syn*-dihydroxylation using osmium tetroxide–*N*-methyl morpholine-*N*-oxide (OsO_4–NMO) (*i.e.* 1,2-diol derivatives: **A** and **B**), (3) periodate-mediated oxidative cleavage of 1,2-diol, followed by *in situ* $NaBH_4$ reduction of di-aldehyde (**B** and **D**; inset in Fig. 2), (4) AgOTf-promoted glycosylation, and (5) global deprotection (see amphiphile synthesis in ESI for details). High diastereomeric purity of all the new detergents was obtained from β-selective glycosylation attained *via* neighboring group participation.[28] Because of the high efficiency of each synthetic step, the final amphiphiles could be prepared with overall yields of ~75%, making preparation of multi-gram quantities of material at a reasonable cost highly feasible. The high purity of the new detergents was confirmed by their individual ^{1}H NMR spectra (Fig. S2$^+$ and S3$^+$). For example, the axial protons of CPM-*C*11 attached to the anomeric carbons, designated H_a, produce two narrowly separated peaks at 4.25 and 4.24 ppm as doublets (Fig. 3b & S2$^+$). But, the same axial protons of the *trans* isomer (*i.e.,* CPM-*T*11) gave two non-separable doublets, located at 4.26 ppm (Fig. 3c & S2$^+$). In addition, these anomeric protons (H_a) of both isomers interact with their neighboring protons (H) with a vicinal coupling constant ($^3J_{aa}$) of 8.0 Hz, revealing that β-selective glycosylation had occurred exclusively. We also observed another doublet peak at 5.16 ppm with a relatively small coupling constant ($^3J_{ae}$ = 4.0 Hz), which corresponds to the α-anomeric protons (H_e) in the terminal glucose units of these detergents (Fig. 3 & S2$^+$).

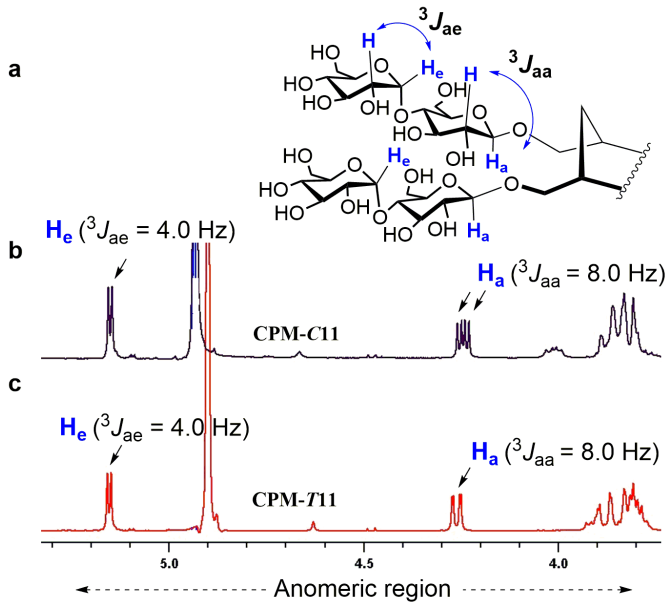

Fig. 3 (a) The chemical structure of the di-maltoside head group of the CPMs is shown to illustrate the anomeric protons of interest (H_e and H_a) and their vicinal couplings with the neighboring protons (H in blue). (b, c) Anomeric regions of the ^{1}H NMR spectra for CPM-*C*11 (b) and CPM-*T*11 (c) showing their high diastereomeric purity (see Fig. S2† for the full range of ^{1}H NMR spectra). Each isomer gave unique spectral features in the anomeric region, indicative of the clear differentiation of the individual isomers by their ^{1}H NMR spectra. Vicinal coupling constants ($^3J_{aa}$ & $^3J_{ae}$) are indicated above individual peaks to differentiatate the α- and β-anomeric protons (H_e and H_a, respectively).

High water-solubility (10 wt %) was found in all four new detergents, yet as for a long alkyl-chain detergent (i.e., CPM-*C*12/*T*12) a brief sonication was required for an initial dissolution (Table 1). Detergent solutions remained clear during a month of incubation at room temperature. Critical micelle concentrations (CMCs) were measured by monitoring dye solubilization using diphenylhexatriene[29] with increasing detergent concentration and the hydrodynamic radii (R_h) of the detergent micelles were estimated through dynamic light scattering (DLS) measurements. The summarized results for the CPMs along with D/X-NBM-C11 and DDM are presented in Table 1. The CMC values of all CPMs (from 0.005 to 0.009 mM) were comparable to those of D/X-NBM-C11, but much smaller than that of DDM (0.170 mM), which indicates the stronger tendencies to form self-assemblies than DDM. Within the same set of detergents (*e.g.,* the CPM-*C*s), the CMC values decreased with increasing alkyl-chain length, due to the increased hydrophobicity. For instance, the CMCs of the CPM-*C*s were lowered from ~0.009 to ~0.006 mM when the alkyl chain length increased from C11 to C12. Micelles formed by the individual sets of detergents were enlarged along with increasing alkyl chain length. Detergent micelle size increased from 4.8 (C11) to 5.5 nm (C12) for the *trans* isomers. Detergent micelle size is determined by the geometry of the detergent molecule, estimated by the volume ratio of detergent head and tail groups.[30] It is interesting to note that the micelle size formed by the *trans* isomers was significantly reduced with change from NB to CP linker. For instance, the R_h value of CPM-*T*11 micelles was 4.8 nm, smaller than X-NBM-C11 (17.3 nm). Even the C12 alkyl chain CPM (CPM-*T*12) formed smaller micelles than X-NBM-C11 with the shorter alkyl chain (5.5 vs 17.3 nm). This comparison reveals that the geometry of the detergent molecules is substantially changed from a cylindrical to a conical shape with the linker modification for the *trans* isomers. This change in detergent geometry likely originates from increased flexibility of the two maltoside head groups, resulting in an increased hydrophilic volume with little affect on the hydrophobic volume (Fig. 1). Interestingly, a different trend was observed for the *cis* isomers. CPM-*C*11/*C*12 were more or less comparable to the D-NBM-C11 in terms of their micelle size (3.8/4.0 vs 3.7 nm). The variation in the conformation of the CP linker (half chair (***C*$_2$**) or envelope (***C*$_s$**)) is likely associated with the different behaviors of the CPM-*C*s and CPM-*T*s in self-assembly formation (Fig. S1†). The DFT calculations show substantial variation in the linker conformation (NB *vs* CP) between D-NBM-C11 and CPM-*C*11, but show little variation in the linker conformation between CPM-*T*11 and X-NBM-C11. The CPM-*C*s formed smaller micelles than the *trans* isomers (i.e., the CPM-*T*s), as exemplified by CPM-*C*11 (3.8 nm) vs CPM-*T*11 (4.8 nm). Our results indicate that a small change in detergent architecture (*i.e.* just eliminating a single C-C bond) can result in a large variation in their self-assemblies, which could also affect detergent efficacy for membrane protein stabilization. When we investigated the size distribution of detergent micelles, all new agents showed only one set of micellar populations in the number- or volume-weighted DLS profiles, indicative of high homogeneity (Fig. S4 & S5†). The appearance of a peak corresponding to large aggregates in the intensity-weighted DLS profiles is likely due to the ultra-sensitivity of light scattering to a large particle.[26] Detergent micelle size was further investigated with increasing temperature (Fig. S6†). DDM gave little change in micelle size with temperature variation from 15 to 65 °C. Consistent with the previous result,[26] the size of the D-NBM-C11 micelles was not affected by temperature, while micelles formed by X-NBM-C11 were substantially enlarged with increasing solution temperature. A similar trend was observed for the CPM analogs (CPM-*C*11 and CPM-*T*11), indicating that micelles formed by the *endo*/*cis* isomer are significantly more stable than the *exo*/*trans* isomer under the conditions. There was little difference in micelle sizes formed by CPM-*C*11 and D-NBM-C11, while micelles formed by CPM-*T*11 were substantially smaller than those formed by X-NBM-C11 over the temperature range tested.

Table 1. Molecular weights (MWs), critical micelle concentrations (CMCs), water-solubility of the novel agents (CPM-*C*s and CPM-*T*s) and control detergents (DDM and X/D-NBM-C11), and hydrodynamic radii (R_h; n = 4) of their micelles in double-distilled water at room temperature.

Detergent	*MW*[a] (Da)	CMC (mM)	CMC (wt%)	R_h (nm)[b]	Solubility (wt%)
CPM-*C*11	1147.4	~ 0.009	~0.0010	3.8±0.04	~10.0
CPM-*C*12	1175.5	~ 0.006	~0.0007	4.0±0.03	~10.0*
CPM-*T*11	1147.4	~ 0.007	~0.0008	4.8±0.03	~10.0
CPM-*T*12	1175.5	~ 0.005	~0.0006	5.5±0.02	~10.0*
X-NBM-C11	1145.4	~ 0.006	~0.0007	17.3±0.10	~5.0*

D-NBM-C11	1145.4	~0.007	~0.0008	3.7±0.05	~5.0
DDM	510.6	~ 0.170	~0.0087	3.4±0.03	>10

[a] Molecular weight of detergents. [b] Hydrodynamic radius of detergent micelles measured at 1.0 wt% detergent concentration by dynamic light scattering. *Sonication required to obtain a clear solution.

As the best protein stabilization efficiency was obtained from CPM-*C*12 (*vide infra*), we carried out in-depth physical characterizations for this agent along with X-NBM-C11 as a reference. X-NBM-C11 and CPM-*C*12 micelles investigated by multi-detection size exclusion chromatography (SEC) showed different distributions when detected using refractive index (RI) and right-angle light scattering (RALS) (Fig. 4). Micelles formed by X-NBM-C11 showed two separated peaks in the SEC profile, indicating a poly-dispersed character for these micelles (Fig. 4a). The peak at 8.4 mL corresponds to an aggregation number (N_{agg}) of between 87 and 183, while the peak at 9.1 mL gives N_{agg} of 183 ~ 751. In contrast, micelles formed by CPM-*C*12 gave a well-defined unimodal distribution, showing only one peak at 9.4 mL, corresponding to N_{agg} of between 60 and 85 (Fig. 4b). This N_{agg} is much smaller than DDM micelles (~ 175). [31] The higher N_{agg} of X-NBM-C11 than that of CPM-*C*12 reflects the bigger micelle size observed by DLS experiment (Table 1).

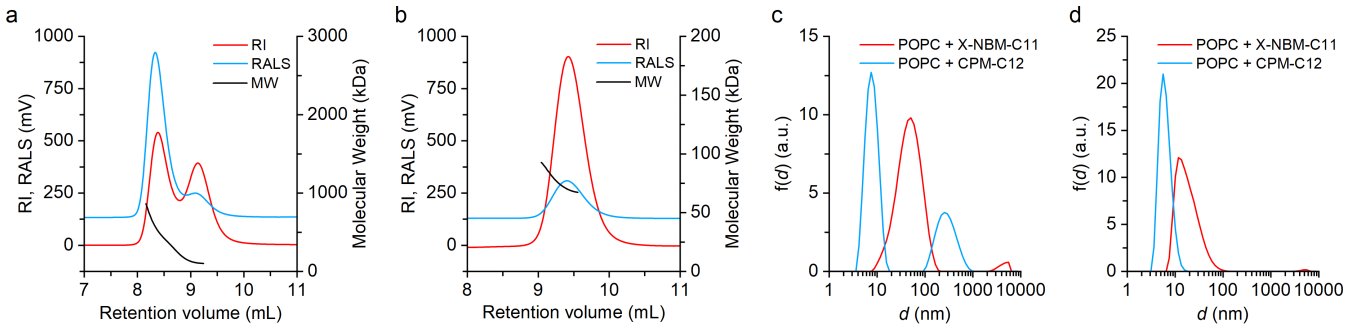

Fig. 4 (a,b) SEC elution and (c,d) DLS profiles for X-NBM-C11 and CPM-*C*12. (a) RI and RALS signals of X-NBM-C11 showed two distinct peaks corresponding to micellar molecular weights ranging from 100 to 210 to 860 kDa. (b) RI and RALS signals of CPM-*C*12 showed a unimodal distribution giving a range of micellar molecular weights from 70 to 100 kDa. (c) Intensity- or (d) volume-weighted DLS profiles for mixtures of either X-NBM-C11 or CPM-*C*12 with POPC vesicles show a major population of small aggregates—most likely mixed lipid-detergent micelles. SEC: size exclusion chromatography; RI: refractive index; RALS: right-angle light scattering.

In order to gain insight into the solubilizing efficiency of the new agents, unilamellar vesicles made of 1-palmitoyl-2-oleoyl-*sn*-glycero-3-phosphocholine (POPC) were separately mixed with 5 mM CPM-*C*12 and X-NBM-C11. Scattering intensity and z-average decreased over incubation time in both detergent cases (Fig S7[†]), thus demonstrating liposome solubilization. Interestingly, the solubilization kinetic of POPC vesicles was faster for CPM-*C*12 than X-NBM-C11. DLS profiles following the liposome solubilization indicate the formation of the small aggregates with hydrodynamic diameters well below the initial size of the POPC vesicles (~120 nm) (Fig. 4c). The volume-weighted size distribution suggested the formation of small assemblies following detergent mixing, with the hydrodynamic diameters close to 5.6 (CPM-*C*12) and 11.7 nm (X-NBM-C11) (Fig. 4d). Based on the liposome solubilization result, these two detergents along with DDM were further tested for extracting diverse membrane proteins from native *Escherichia coli* (*E. coli*) membranes. Of the tested detergents, CPM-*C*12 was most efficient at extracting *E. coli* membrane proteins of various sizes, followed by X-NBM-C11 and DDM (Fig. 5).

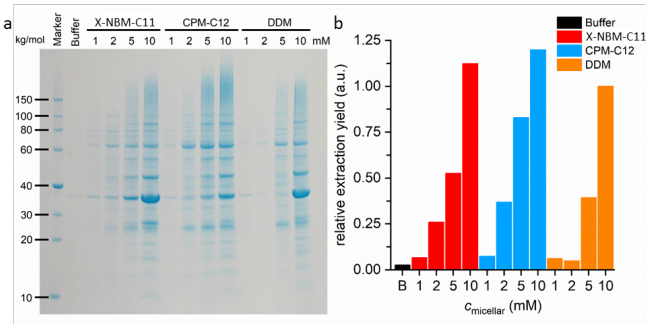

Fig. 5 (a) SDS-PAGE of detergent-solubilized fractions and (b) calculated protein extraction yields of CPM-*C*12 from the native *E. coli* membranes. X-NBM-C11 and DDM were used as positive controls. Cell membrane fragments from *E. coli* BL21 (DE3) were incubated with three individual detergents (X-NBM-C11, CPM-*C*12, and DDM) for 16 hrs at four different concentrations (1, 2, 5, and 10 mM). Band intensity in each lane was measured by densitometry using imageJ.

Detergent evaluation with diverse model membrane proteins

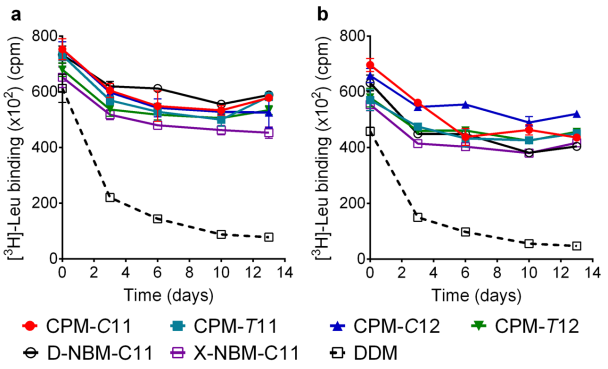

Fig. 6 Long-term stability of LeuT solubilized in CPMs (CPM-*C*11/*T*11/*C*12/*T*12) at the two detergent concentrations: (a) CMCs + 0.04 wt % and (b) CMCs + 0.2 wt %. X/D-NBM-C11 and DDM were used as positive controls. Ligand binding activity of the transporter was measured using a radio-labeled substrate ([^{3}H]-Leucine (Leu)) at regular intervals during a 13-day incubation at room temperature. LeuT activity was measured *via* scintillation proximity assay (SPA). Error bars, SEM, *n* = 3.

To assess the potential utility of new amphiphiles as tools for membrane protein study, we evaluated several model protein systems with the CPMs, using DDM and X/D-NBM-C11 as controls. The suitability of the isomeric CPMs (CPM-*C*s and CPM-*T*s) for membrane protein study was first investigated with the bacterial leucine transporter (LeuT), a prokaryotic homologue of the mammalian neurotransmitter/Na$^+$ symporters (NSSs family) from *Aquifex aeolicus*.[32,33] This transporter was initially extracted from the membranes with 1.0 wt% DDM and purified in 0.05 wt% of the same detergent. The DDM-purified LeuT was diluted into buffer solutions containing individual agents (CPM-*C*11/*C*12, CPM-*T*11/*T*12, D/X-NBM-C11, or DDM) to reach final detergent concentrations of CMCs + 0.04 wt % or CMCs + 0.2 wt%. We assessed protein stability by measuring radiolabeled leucine ([^{3}H]-Leu) binding *via* scintillation proximity assay (SPA)[34] at regular intervals during a 13-day incubation at room temperature. At both detergent concentrations, the DDM-solubilized LeuT underwent a gradual loss of protein activity over the incubation period (Fig. 6). Consistent with a previous result,[26] X/D-NBM-C11 was markedly superior to DDM in terms of preserving the functional state of the transporter. All CPMs were more or less comparable to X/D-NBM-C11 at maintaining transporter activity (Fig. 6a,b). No clear difference between the isomers (*i.e.* CPM-*C*s *vs* CPM-*T*s) was observed in this regard although the *cis* isomers look slightly better than the *trans* isomers. This result suggests that overall the CPM architecture is favorable for LeuT stability long term. There was little observed differences in stability of the LeuT in the CPM agents with different stereo-chemistry.

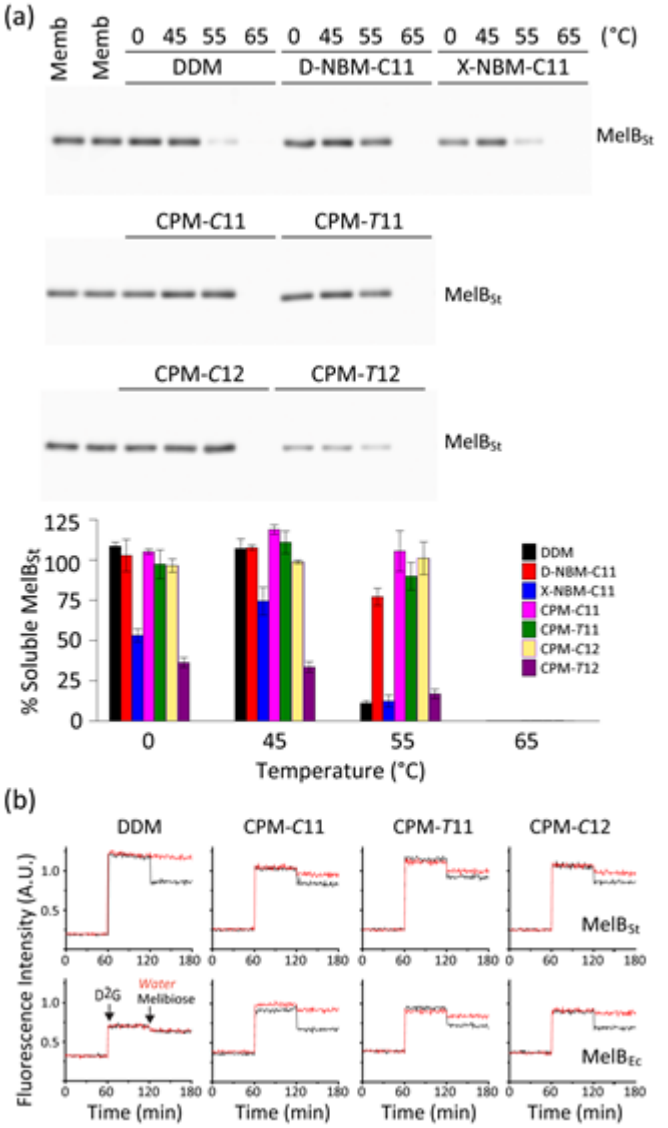

Fig. 7 (a) Thermo-solubility of MelB$_{St}$ solubilized in four CPM agents. DDM and D/X-NBM-C11 were used as controls. MelB$_{St}$ was extracted from *E. coli* membranes using 1.5 wt % individual detergents for 90 min at 0 °C. These detergent extracts were further incubated for another 90 min at an elevated temperature (45, 55 or 65 °C). Following ultracentrifugation to remove insoluble protein and cellular debris, the soluble MelB$_{St}$ was separated by SDS-PAGE and visualized by Western blot (*top panel*). The amount of soluble MelB$_{St}$ was expressed as a percentage of total MelB$_{St}$ in the untreated membrane (Memb) and presented as a histogram (a, *bottom panel*). Error bars, SEM, *n* = 2. (b) Galactoside binding-mediated FRET reversal. Right-side-out (RSO) membrane vesicles containing MelB$_{St}$ or MelB$_{Ec}$ were solubilized with DDM, CPM-*C*11, CPM-*T*11, or CPM-*C*12. The detergent extracts were used to measure melibiose reversal of FRET from Trp to dansyl-2-galacotside (D^{2}G). D^{2}G at 10 µM and melibiose at a saturating concentration were added at 1 min and 2 min time points, respectively (black lines). Control data (red lines) were obtained by addition of water instead of melibiose.

The new agents were further investigated for the extraction and stabilization of melibiose permease from *Salmonella typhimurium* (MelB$_{St}$).[35] *E. coli* membrane fractions containing MelB$_{St}$ were treated with 1.5 wt% of individual detergents (DDM, D/X-NBM-C11, or CPM-

*C*11/*T*11/*C*12/*T*12) for 90 min at 0 °C and the resulting detergent extracts were further incubated at an elevated temperature (45, 55 or 65 °C) for another 90 min. The amounts of soluble $MelB_{St}$ under the tested conditions were quantified by Western blot analysis and expressed as percentages of the initial amount of $MelB_{St}$ present in the untreated membranes. As a mild detergent is unlikely to destroy transporter integrity at a low temperature, the amount of soluble $MelB_{St}$ obtained at 0 °C would mainly reflect detergent extraction efficiency. If detergent-extracted $MelB_{St}$ is further treated at a high temperature of 45, 55, or 65 °C, the amount of soluble $MelB_{St}$ depends on detergent ability to prevent protein aggregation under the conditions tested. Consistent with a previous result,[26] X-NBM-C11 failed to solubilize $MelB_{St}$, while its *endo* isomer (D-NBM-C11) was efficient in this regard (Fig. 7a). DDM and D-NBM-C11 quantitatively extracted the transporter at 0 °C. Similar efficiencies for protein solubilization (90−100%) were observed for the CPM agents with the exception of CPM-*T*12. CPM-*T*12 was similar to X-NBM-C11 in terms of $MelB_{St}$ extraction efficiency. At an elevated temperature of 45 °C, the amounts of soluble $MelB_{St}$ were more or less similar to those observed at 0 °C. When the incubation temperature was further increased to 55 °C, however, detergent efficacy for $MelB_{St}$ solubilization was clearly differentiated. At this high temperature, DDM and X-NBM-C11 gave only ~10% soluble $MelB_{St}$, while D-NBM-C11 yielded 75% solubilized $MelB_{St}$. CPM-*T*12 was inferior to D-NBM-C11, but the other three CPMs (CPM-*C*11, CPM-*T*11 and CPM-*C*12) were more effective than DDM at maintaining MelB solubility, with the best performance observed for CPM-*C*11 and CPM-*C*12 (~100%). This result indicates that these CPM agents were not only efficient at extracting the transporter, but also effective at preserving the transporter in a soluble state upon heating. Additionally, the CPM-*C*s appeared to be superior to the *trans* isomers (CPM-*T*s) at maintaining $MelB_{St}$ in a soluble form. To further evaluate relative detergent effectiveness to DDM, the three CPMs (CPM-*C*11, CPM-*T*11 and CPM-*C*12) were selected for $MelB_{St}$ functional assay. $MelB_{St}$ function was assessed by melibiose reversal of Förster resonance energy transfer (FRET) from tryptophan to 2'-(*N*-dansyl)aminoalkyl-1-thio-β-D-galactopyranoside (D^2G).[35a,d,e] An active transporter binds to both fluorescent galactoside ligand (D^2G) and non-fluorescent substrate (melibiose). Consequently, D^2G addition to active $MelB_{St}$ gives a strong florescent signal that could be reversed by addition of a competitive melibiose as a ligand−substrate exchange occurs in the binding pocket. The DDM-solubilized $MelB_{St}$ showed a response to the addition of both D^2G and melibiose (Figure 7b). However, a complete loss in transporter function was observed when a less stable homologue, $MelB_{EC}$ obtained from *E. coli*, was used under the same conditions.[35d] In contrast, all the tested CPMs (CPM-*C*11, CPM-*T*11 and CPM-*C*12) preserved the functionality of both MelB homologues. Collectively, these three CPMs were superior to DDM at maintaining MelB in a soluble and functional form.

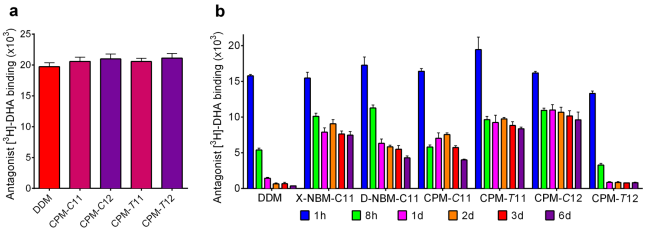

Fig. 8 (a) Initial or (b) long-term ligand binding ability of β_2AR solubilized in individual detergents (DDM, CPM-*C*s and CPM-*T*s). DDM and X/D-NBM-C11 were used as positive controls. DDM-purified receptor was diluted into buffer solutions containing the individual new agents or DDM/CHS to reach the final detergent concentrations of CMCs + 0.2 wt %. Ligand binding activity of the receptor was measured using radio-labelled ligands ([^{3}H]-dihydroalprenolol (DHA)). Receptor activity was measured following 30-min dilution (a) or at regular intervals during a 6-day incubation (b) at room temperature. Error bars, SEM, n = 3.

We next assessed the new agents using a GPCR, the human β_2 adrenergic receptor (β_2AR).[36] The receptor was first extracted and purified using DDM. The DDM-purified receptor was diluted in buffer solutions supplemented with either the new individual agents without cholesteryl hemisuccinate (CHS) or DDM with CHS. The final detergent concentration was 0.2 wt% for all tested detergents. As a direct assessment of receptor stability, the ability of the receptor to bind the radioactive antagonist ([^{3}H]-dihydroalprenolol (DHA)) was measured.[37-39] A preliminary result was obtained by measuring the ligand binding ability of the receptor following 30-min sample dilution. All CPM agents were as effective as DDM at maintaining receptor activity (Fig. 8a). In order to further investigate detergent efficacy, ligand binding activity of the receptor solubilized in the individual detergents was monitored at regular intervals over a 6-day incubation at room temperature (Fig. 8b). The DDM-solubilized receptor showed high initial activity, but rapidly lost its activity, giving only ~5% residual activity at the end of the incubation. A similar trend was observed for CPM-*T*12. X/D-NBM-C11-solubilized receptor retained approximately 50/30% of the initial activity at day 6. There is little difference in β_2AR stabilization between the CPMs and NBMs, as exemplified by CPM-*C*11 vs D-NBM-C11 and CPM-*T*11 vs X-NBM-C11. CPM-*C*12-solubilized receptor showed the highest retention in receptor activity over the incubation period (Fig. 8b).

The promising results with LeuT, MelB and β_2AR prompted us to select three CPMs (CPM-*C*11, CPM-*C*12 and CPM-*T*11) for the further evaluation with another GPCR, mouse μ-opioid receptor (MOR).[40] The individual detergents were used at 0.5 wt%. MOR stability was assessed by measuring receptor T_m via CPM assay. Along with DDM, LMNG, widely used for GPCR study, was included as a control in detergent evaluation. As expected, LMNG-solubilized MOR gave 5.7 °C higher T_m than DDM-solubilized receptor (28.0 vs 33.7 °C) (Fig. 9). CPM-*T*11 was comparable to LMNG at stabilizing the receptor, while the *cis* isomers (CPM-*C*11 an CPM-*C*12) were notably more effective than LMNG. MOR solubilized in CPM-*C*11 and CPM-*C*12 gave T_ms of 36.3 and 39.3 °C, respectively. Receptor T_m was further increased by 5.6 °C when solubilized in CPM-*C*12 instead of LMNG, indicating the promise of this agent for GPCR structural study, particularly when combined with the β_2AR result.

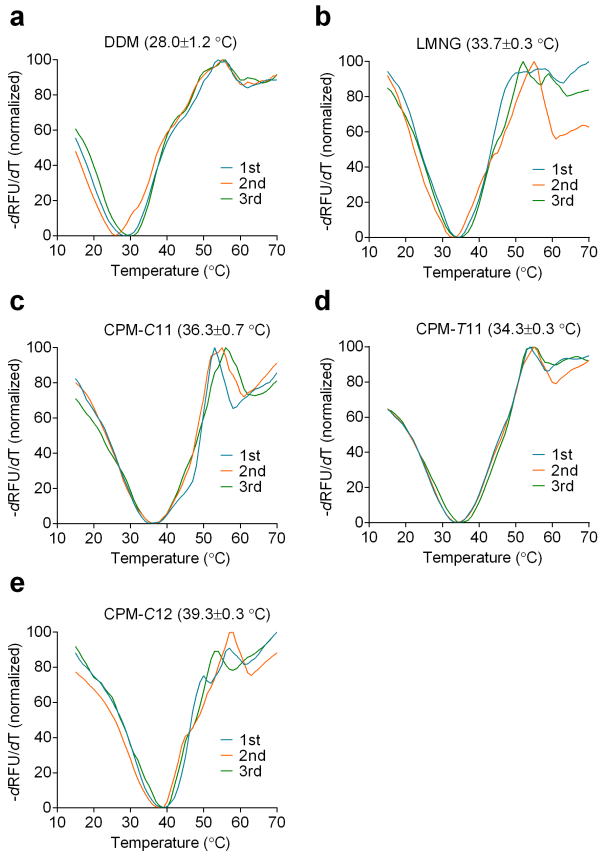

Fig.9 Melting temperatures (T_m) of MOR solubilized in the designated detergents and derivative functions (normalized) of CPM profiles. T_m values were obtained from the derivative functions of the CPM profiles. For CPM assay, the receptor was solubilized in DDM (a), LMNG (b), CPM-*C*11 (c), CPM-*T*11 (d), and CPM-*C*12 (e) and temperatures of individual samples were increased from 15 to 70 °C. The value in parenthesis represents average receptor T_m ± SEM (n = 3).

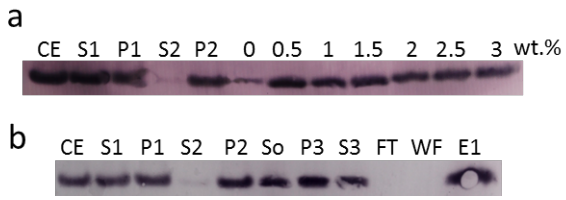

Fig. 10 Western blot analysis of prokaryotic voltage-dependent potassium channel (KvAP) over (a) *E. coli* XL-1 Blue membrane preparation and solubilization and (b) extraction and purification of the channel protein by immobilized metal affinity chromatography (IMAC) using Talon Co^{2+} beads. CPM-*C*12 was used at seven different concentrations (0, 0.5, 1, 1.5, 2, 2.5 and 3 wt %) (a) or 1.0 wt % (b) for KvAP extraction. **CE**: crude extract; **S1** and **P1**: supernatant and pellet after the first centrifugation (6000 *g*); **S2** and **P2**: supernatant and pellet after the second centrifugation (100,000 *g*); **So**: solubilized material; **S3** and **P3**: supernatant and pellet after the third centrifugation (100,000 *g*); **FT**: flow through; **WF**: washed fraction; **E1**: eluted fraction.

As CPM-*C*12 was most effective at stabilization of multiple membrane proteins, we investigated whether this agent can be effectively used for protein extraction/solubilization and purification of a prokaryotic voltage-dependent potassium channel (KvAP) cloned from *Aeropyrum pernix* and expressed in E.coli?.[41] Whole cells were subjected to alkaline lysis, followed by two-step centrifugation (6,000 and 100,000 *g*) and the resulting KvAP-containing membranes were incubated with CPM-*C*12 at a range of concentrations from 0 to 3.0 wt% for three hours at room temperature. The amounts of solubilized KvAP under the conditions were estimated by SDS-PAGE (Fig S8) and Western blot (Fig 10a). CPM-*C*12 was efficient at KvAP extraction and solubilization, and the amount of solubilized KvAP showed little dependency on detergent concentration over the range of 0.5 to 3.0 wt% tested. In order to explore the utility of this detergent for protein purification, the KvAP channel was extracted and solubilized using 1.0 wt% CPM-*C*12. The resulting detergent-solubilized channel was loaded onto immobilized metal affinity chromatography (IMAC) for purification. CPM-*C*12-purified KvAP was obtained by adding 1.5 column volumes of elution buffer containing 0.25 wt% CPM-*C*12 and 400 mM imidazole at pH 8.0. The eluted sample yielded detectable amounts of KvAP (Fig 10b and Fig. S9[†]). Combined together, these results indicate that CPM-*C*12 can be effectively used for membrane protein extraction and purification.

Discussion

Membrane proteins have different tendencies to denature/aggregate in solution due to large variations in the structures and properties. This is the reason why we lack a magic bullet detergent suitable for working with all membrane proteins. Despite the protein-specific nature of detergent efficacy for protein stabilization, DDM is widely used for membrane protein research, and thus is an accepted gold standard for membrane protein structural study. In the current study, we developed a novel class of diastereomeric amphiphiles (CPMs) based on our previous NBM study and evaluated their efficacy for protein stabilization with multiple membrane proteins (LeuT, MelB, β_2AR, and MOR). The best detergent was CPM-*C*12, markedly superior to DDM for all the membrane proteins tested here. In addition, this C12 alkyl-chained CPM was even better than X/D-NBM-C11 at stabilizing the membrane proteins. When compared with LMNG, a particularly optimized detergent for GPCR stability, CPM-*C*12 was notably better than this NG class detergent for stabilization of two GPCRs (β_2AR and MOR). CPM-*C*12 was better at stabilizing β_2AR than X-NBM-C11, an agent shown previously to be better than LMNG at stabilizing the receptor in our previous NBM study.[26] CPM-*C*12 gave 5.6 °C higher T_m of the receptor than LMNG in the case of MOR. Furthermore, CPM-*C*12 was efficient at extracting membrane proteins ($MelB_{St}$) and successfully used for both solubilization and purification of the channel protein (KvAP). Thus, these results reveal that this CPM will find wide use in studying membrane proteins, particularly for GPCRs. Development of such detergents with enhanced protein stabilization efficacy and good protein extraction efficiency is challenging as multiple detergent properties need to be individually optimized within a single small architecture.

It is important to identify the structural feature responsible for superiority of CPM-*C*12 compared to X/D-NBM-C11 at protein stabilization. These detergents (CPM-*C*12 vs X/D-NBM-C11) mainly differ in the core structure (CP/NB) and alkyl chain length (C11/C12). In order to explore the effect of the detergent core unit on protein stability, it is necessary to compare detergent efficacy between a pair of detergents with the same alkyl chain length and the same relative configuration of detergent head and tail groups (e.g., CPM-*C*11 vs D-NBM-C11). CPM-*C*11 was more or less comparable to D-NBM-C11 at stabilizing the membrane proteins (LeuT, $MelB_{St}$ and β_2AR). A similar trend was observed for the *trans/exo* versions (CPM-*T*11 *vs* X-NBM-C11), with the exception of $MelB_{St}$ stability. This comparison indicates that the presence of a CP rather than an NB core is unlikely to be responsible for the favorable protein stabilization behavior of the CPMs compared to the NBMs. In other words, the increase in the hydrophilic group flexibility attained by the introduction of the CP core is not a *direct* reason for the enhanced protein stabilization efficacy of CPM-*C*12 relative to X/D-NBM observed here. Rather, the increased hydrophilic group flexibility appears to give an *indirect* effect on protein stability as it conferred enhanced water-solubility to the CPM molecules, allowing for preparation of a water-soluble detergent with C12 alkyl chain length (i.e., CPM-*C*12). As a result, we conceive that CPM-*C*12 is optimal for protein stabilization not because of enhanced flexibility of this CPM in the hydrophilic region, but because of the possession of the alkyl chain (i.e., C12) more compatible with the hydrophobic dimensions of protein surfaces compared to D/X-NBM-C11. At first glance, this conclusion seems inconsistent with the general concept that detergent flexibility is critical for membrane protein stabilization.[42,31,43] However, such detergent flexibility is associated with detergent hydrophobic group rather than hydrophilic group. Thus, the current result is still compatible with the previous results, yet implies a distinctive role for detergent flexibility associated with the head group in protein stability.

It is interesting to compare the *cis* and *trans* versions of CPMs in terms of protein stabilization as this configuration difference generates variation in a relative direction of the detergent head and tail groups. The relative efficacy of the CPM-*C*s and CPM-*T*s for protein stabilization was dependent on detergent alkyl chain length (C11/C12) and a target membrane protein (MelB, MOR, LeuT or β_2AR). In the cases of C11 versions, the *cis*-configured CPM (CPM-*C*11) was slightly better than the *trans* isomer (CPM-*T*11) for MelB and MOR stability, while an opposite trend was observed for β_2AR stability. When it comes to the C12 versions, CPM-*C*12 was clearly superior to CPM-*T*12 at stabilizing MelB and β_2AR, while little difference was observed for LeuT stability. Thus, there was no clear-cut trend of detergent efficacy between the CPMs with the *cis* and *trans* configurations. However, the CPM-*C*s showed overall favorable behaviors for stabilizing the membrane proteins compared to the *trans* counterparts. The general outperformance of the *cis* isomers compared to the *trans* isomers is likely associated with a difference in conformation of the CP core unit (half-chair or envelope) between these stereoisomers. The conformation of the CP ring not only determines the relative directions of the alkyl chains and two maltose groups, but also affects detergent hydrophobic length and molecular symmetry. Alternatively, the enhanced thermal stability of detergent micelles could be associated with the favorable behaviors of the *cis* isomers compared to the *trans* counterparts (Fig. S6).

Conclusions

With variations of stereochemistry and alkyl chain length we report herein two sets of diastereomeric cyclopentane-based maltosides. Of the new agents, we identified CPM-*C*12 that was markedly more effective than optimized novel detergents (X-NBM-C11 and LMNG) as well as a gold standard detergent (DDM) at stabilizing the GPCRs. A successful extraction and purification of a challenging voltage-gated potassium channel (KvAP), along with the efficient solubilization of $MelB_{St}$ and *E. coli* membrane proteins, would further increase the utility of this agent. Hence, this CPM represents an invaluable tool for membrane protein structural study. Additionally, detergent comparison enabled us to propose roles for both detergent flexibility associated with the hydrophilic group and detergent core conformation in protein stability, which will assist rational design of novel detergents in future.

Conflict of interest

The authors declare the following competing financial interest(s): P.S.C. and M.D. are co-inventors on a patent application that covers the CPM agents.

Acknowledgements

This work was supported by the National Research Foundation of Korea (NRF) (2016R1A2B2011257 and 2018R1A6A1A03024231 to P.S.C.). We acknowledge Julia Lenz for preparing native *E. coli* membranes for extraction studies. This study was also supported by the National Institutes of Health (grants R01GM122759 and R21NS105863 to L.G.).

Notes and references

1 a) Sanders, C. R.; and Myers, J. K. Disease-related misassembly of membrane proteins *Annu. Rev. Biophys. Biomol. Struct*., **2004**, *33*, 25–51; b) Overington, J. P.; Al-Lazikani, B.; and Hopkins, A. L. How many drug targets are there? *Nat. Rev. Drug Discovery*, **2006**, *5*, 993–996.

2 Membrane proteins of known 3D structure, http://blanco.biomol.uci.edu/mpstruc

3 Kuhlbrandt, W. Microscopy: cryo-EM enters a new era. *Elife* **2014**, *3*, e03678.

4 (a) Garavito, R. M.; and Ferguson-Miller, S. Detergents as tools in membrane biochemistry. *J. Biol. Chem*., **2001**, *276*, 32403–32406; (b) Serrano-Vega, M. J.; Magnani, V.; Shibata, Y.; and Tate, C. G. Co-evolving stability and conformational homogeneity of the human adenosine A2a receptor. *Proc. Natl. Acad. Sci. U. S. A*., **2008**, *105*, 10744–10749.

5 (a) Newstead, S.; Ferrandon, S.; and Iwata, S. Rationalizing α-helical membrane **protein** crystallization. *Protein Sci*., **2008**, *17*, 466–472; (b) He, Y.; Wang, v,; and Yan, N. The recombinant expression systems for structure determination of eukaryotic membrane **proteins**. *Protein Cell*, **2014**, *5*, 658–672; (c) Parker, J. L.; and Newstead, S. Current trends in α-helical membrane **protein** crystallization. *Protein Sci*., **2012**, *21*, 1358–1365.

6 Israelachvili, J .N.; Mitchell, D. J.; and Ninham, B. W. Theory and self-assembly of lipid bilayers and vesicles. *Biochim. Biophys. Acta, Biomembr*. **1977**, *470*, 185-201.

7 Chaptal, V.; et al., Quantification of detergents complexed with membrane proteins. *Sci. Rep*. **2017**, *7*, 41751.

8 Loll, P. J. Agrobacterium: from **biology** to biotechnology. *J. Struct. Biol.* **2003**, *142*, 144–153. (b) White, S. H. The progress of membrane **protein** structure determination. *Protein Sci.* **2004**, *13*, 1948–1949.

9 Nath, A.; Atkins, W. M.; Sligar, S. G. Applications of phospholipid bilayer nanodiscs in the study of membranes and membrane proteins. *Biochemistry.* **2007**, *46*, 2059−2069.

10 (a) Broecker, J.; Eger, B. T.; Ernst, O. P. Crystallogenesis of membrane proteins mediated by polymer-bounded lipid nanodiscs. *Structure* **2017**, *25*, 384−392. (b) Oluwole, A. O.; Danielczak, B.; Meister, A,.' Babalola, J. O.; Vargas, C.; Keller, S.; Solubilization of membrane proteins into functional lipid-bilayer nanodiscs by diisobutylene/maleic acid copolymer. *Angew. Chem. Int. Ed.* **2017**, *56*, 1919.

11 (a) Tribet, C.; Audebert, R.; Popot, J.-L. Amphipols: polymers that keep membrane proteins soluble in aqueous solutions. *Proc. Natl. Acad. Sci. U. S. A.* **1996**, *93*, 15047−15050. (b) Popot, J. L.; Althoff, T.; Bagnard, D.; Banères, J. L.; Bazzacco, P.; Billon-Denis, E.; Crémel, G. Amphipols from A to Z. *Annu. Rev. Biophys*. **2011**, *40*, 379−408.

12 Tao, H.; Lee, S. C.; Moeller, A.; Roy, R. S.; Siu, F. Y.; Zimmermann, J.; Zhang, Q. Engineered nanostructured β-sheet peptides protect membrane proteins. *Nat. Methods* **2013**, *10*, 759.

13 (a) McGregor, C.-L.; Chen, L.; Pomroy, N. C.; Hwang, P.; Go, S.; Chakrabartty, A.; Privé, G. G. Lipopeptide detergents designed for the structural study of membrane proteins. *Nat. Biotechnol*. **2003**, *21*, 171. (b) Guettou, F., Moberg, P., Zhu, L., Jegerschöld, C., Flayhan, A., Briggs, J. A. and Garoff, H. A saposin-lipoprotein nanoparticle system for membrane proteins. *Nature methods,* **2016,** *13*, 345-351

14 (a) Chae, P. S.; Rasmussen, S. G.; Rana, R. R.; Gotfryd, K.; Chandra, R.; Goren, M. A.; Kruse, A. C.; Nurva, S.; Loland, C. J.; Pierre, Y. Maltose−neopentyl glycol (MNG) amphiphiles for solubilization, stabilization and crystallization of membrane proteins. *Nat. Methods* **2010**, *7*, 1003. (b) Chae, P. S.; Rana, R. R.; Gotfryd, K.; Rasmussen, S. G.; Kruse, A. C.; Cho, K. H.; Gether, U. Glucoseneopentyl glycol (GNG) amphiphiles for membrane protein study. *Chem. Commun*. **2013**, *49*, 2287−2289. (c) Cho, K. H.; Husri, M.; Amin, A.; Gotfryd, K.; Lee, H. J.; Go, J.; Chae, P. S. Maltose neopentyl glycol-3 (MNG-3) analogues for membrane protein study. *Analyst* **2015**, *140*, 3157−3163. (d) Bae, H. E.; Du, Y.; Hariharan, P.; Mortensen, J. S.; Kumar, K. K.; Ha, B.; Kobilka, B. K. Asymmetric maltose neopentyl glycol amphiphiles for a membrane protein study: effect of detergent asymmetricity on protein stability. *Chem. Sci*. **2019**, *10*, 1107−1116.

15 Hussain, H.; Du, Y.; Scull, N. J.; Mortensen, J. S.; Tarrasch, J.; Loland, C. J.; Byrne, B.; Kobilka, K.; Chae, P. S. Accessible mannitol-based amphiphiles (MNAs) for membrane protein solubilization and stabilization. *Chem. Eur. J.* **2016,** *22,* 7068 –7073.

16 Chae, P. S.; Kruse, A. C.; Gotfryd, K.; Rana, R. R.; Cho, K. H.; Rasmussen, S. G.; Bae, H. E.; Chandra, R.; Gether, U.; Guan, L. Novel tripod amphiphiles for membrane protein analysis. *Chem. - Eur. J.* **2013**, *19*, 15645−15651.

17 Matar-Merheb, R.; Rhimi, M.; Leydier, A.; Huché, F.; Galián. C,.; Desuzinges-Mandon, E.; Ficheux, D.; Flot, D.; Aghajari, N.; Kahn, R.; Di Pietro, A.; Jault, J. M.; Coleman, A. W.; Falson, P. Structuring detergents for extracting and stabilizing functional membrane proteins. *PLoS One*. **2011**, *6*, e18036.

18 Hussain, H.; Mortensen, J. S.; Du, Y.; Santillan, C.; Ribeiro, O.; Go, J.; Hariharan, P.; Loland, C. J.; Guan, L.; Kobilka, B. K.; Byrne, B.; Chae, P. S. Tandem malonate-based glucosides (TMGs) for membrane protein structural studies. *Sci. Rep*. **2017**, *7*, 3963.

19 Ehsan, M.; Du, Y.; Scull, N. J.; Tikhonova, E.; Tarrasch, J.; Mortensen, J. S.; Loland, C. J.; Skiniotis, G.; Guan, L.; Byrne, B. Highly branched pentasaccharide-bearing amphiphiles for membrane protein studies. *J. Am. Chem. Soc.* **2016**, *138*, 3789−3796.

20 Das, M.; Du, Y.; Mortensen, J. S.; Ribeiro, O.; Hariharan, P.; Guan, L.; Loland, C. J.; Kobilka, B. K.; Byrne, B.; Chae, P. S. Butane-1, 2, 3, 4-tetraol-based amphiphilic stereoisomers for membrane protein study: importance of chirality in the linker region. *Chem. Sci*. **2017**, *8*, 1169−1177.

21 Nguyen, K. A,; Peuchmaur, M.; Magnard, S.; Haudecoeur, R.; Boyère, C,.; Mounien, S,.; Benammar, I.; Zampieri, V.; Igonet, S.; Chaptal, V,.; Jawhari, A.; Boumendjel, A.; Falson, P. Glycosyl-Substituted Dicarboxylates as Detergents for the Extraction, Overstabilization, and Crystallization of Membrane Proteins. *Angew. Chem. Int. Ed*. **2018**, *57*, 2948-2952.

22 Sadaf, A.; Du, Y.; Santillan, C.; Mortensen, J.; Molist, I.; Seven, A.; Hariharan, P.; Skiniotis, G.; Loland, C.; Kobilka, B. K.; Guan, L.; Byrne, B.; Chae, P. S. Dendronic trimaltose amphiphiles (DTMs) for membrane protein study. *Chem. Sci*. **2017**, *8*, 8315−8324.

23 Ghani, L.; Munk, C. F.; Zhang, X.; Katsube, S.; Du, Y.; Cecchetti, C.; Huang, W.; Bae, H. E.; Saouros, S.; Ehsan, M.; Guan, L.; Liu, X.; Loland, C. J.; Kobilka, B. K.; Byrne, B.; and Chae, P. S. 1,3,5-Triazine-Cored Maltoside Amphiphiles for Membrane Protein Extraction and Stabilization. *J. Am. Chem. Soc*. **2019**, *141*, 19677−19687.

24 (a) Rasmussen, S. G. F.: et al., Structure of a nanobody-stabilized active state of the β_2 adrenoceptor. *Nature*, **2011**, *469*, 175–180; (b) Kruse, A. C.; et al., Activation and allosteric modulation of a muscarinic acetylcholine receptor. *Nature*, **2012**, 482, 552–556; (c) Manglik, A.; Kruse, A. C.; Kobilka, T. S.; Thian, F. S.; Mathiesen, V.; Sunahara, R. K.; Pardo, L.; Weis, W. I.; Kobilka, B. K.; and Granier, S. Crystal structure of the μ-opioid receptor bound to a morphinan antagonist. *Nature*, **2012**, *485*, 321–326; (d) Ring, A. M.; Manglik, A.; Kruse, A. C.; Enos, M. D.; Weis, W. I.; Garcia, K. C.; Kobilka, B. K. Adrenaline-activated structure of β2-adrenoceptor stabilized by an engineered nanobody. *Nature*, **2013**, *502*, 575–579; (e) Miller, V.; and Aricescu, A. R. Crystal structure of a human GABAA receptor. *Nature*, **2014**, *512*, 270– 275; (f) Karakas, E.; and Furukawa, H. Crystal structure of a heterotetrameric NMDA receptor ion channel. *Science*, **2014**, *344*, 992–997; (g) Suzuki, H.; Nishizawa, T.; Tani, K.; Yamazaki, Y.; Tamura, A.; Ishitani, R.; Dohmae, N.; Tsukita, S.; Nureki, O.; and Fujiyoshi,, Y. Crystal Structure of a Claudin Provides Insight into the Architecture of Tight Junctions. *Science*, **2014**, *344*, 304–307; (h) Frick, A.; Eriksson, U. K.; De Mattia, F.; Oberg, F.; Hedfalk, K.; Neutze, R.; Grip, W. J.; Deen, P. M. T.; and TornrothHorse, S. X-ray structure of human aquaporin 2 and its implications for nephrogenic diabetes insipidus and trafficking. *Proc. Natl. Acad. Sci. U. S. A*., **2014**, *111*, 6305– 6310; (i) Yin, J.; Mobarec, J.C.; Kolb, P.; and Rosenbaum, D. M. Crystal structure of the human OX2 orexin receptor bound to the insomnia drug suvorexant. *Nature*, **2015**, *519*, 247–250; (j) Kang,Y.; Zhou, X. E.; et al., Crystal structure of rhodopsin bound to arrestin by femtosecond X-ray laser. *Nature*, **2015**, *523*, 561–567; (k) Perez, C.; Gerber, S.; Boilevin, J.; Bucher, M.; Darbre, T.; Aebi, M.; Reymond, J.-L.; and Locher, K. P. Structure and mechanism of an active lipid-linked oligosaccharide flippase. *Nature*, **2015**, *524*, 433– 438; (l) Taniguchi, R.; Kato, H. E.; Font, J.; Deshpande, C. N.; Wada, M.; Ito, K.; Ishitani, R.; Jormakka, M. and Nureki, O. Outward- and inward-facing structures of a putative bacterial transition-metal transporter with homology to ferroportin. *Nat. Commun*., **2015**, *13*, 8545; (m) Dong, Y. Y.; et al., K2P channel gating mechanisms revealed by structures of TREK-2 and a complex with Prozac. *Science*, **2015**, *347*, 1256–1259; (n) Paulsen, C. E.; Armache, J.-P.; Gao, Y.; Cheng, Y. and Julius D., Structure of the TRPA1 ion channel suggests regulatory mechanisms. *Nature*, **2015**, *520*, 511–517. (n) Kellosalo, J.; Kajander, T.; Kogan, K.; Pokharel, K.; Goldman, A. The structure and catalytic cycle of a sodium-pumping pyrophosphatase. *Science* **2012**, *337*, 473−476.

25 (a) Zhang, Q.; X. Ma, A. Ward, W.-X. Hong, V.-P. Jaakola, R. C. Stevens, M. G. Finn, G. Chang, Designing facial amphiphiles for the stabilization of integral membrane proteins. *Angew. Chem., Int. Ed*. **2007**, *46*, 7023–7025; (b) Lee, S. C.; Bennett, B. C.; Hong, W.-X.; Fu, Y.; Baker, K. A.; Marcoux, J.; Robinson, C. V.; Ward, A. B.; Halpert, J. R.; Stevens, R. C.; Stout, C. D.; Yeager, M. J.; Zhang, Q.; *Proc. Natl. Acad. Sci. U. S. A.* **2013**, *110*, E1203−E1211; (c) Das, M.; Du, Y.; Mortensen, J. S.; Bae, H. E.; Byrne, B.; Loland, C. J.; Kobilka, B. K. and Chae, P. S. An engineered lithocholate-based facial amphiphile stabilizes membrane proteins: assessing the impact of detergent customizability on protein stability. *Chem. Eur. J.* **2018**, *24*, 9860.

26 Das, M.; Du, Y.; Ribeiro, O.; Hariharan, P.; Mortensen, J. S.; Patra, D.; Byrne, B. Conformationally preorganized diastereomeric norbornane-

based maltosides for membrane protein study: Implications of detergent kink for micellar properties. *J. Am. Chem. Soc.* **2017**, *139*, 3072−3081.

27 Chae, P. S.; Kruse, A. C.; Gotfryd, K.; Rana, R. R.; Cho, K. H.; Rasmussen, S. G. F.; Bae, H. E.; Chandra, R.; Gether, U.; Guan, L.; Kobilka, B. K.; Loland, C. J.; Byrne, B.; and Gellman, S. H. Novel tripod amphiphiles for membrane protein analysis. *Chem.–Eur. J.,* **2013**, *19*, 15645–15651.

28 Veeneman, G.H.; Leettwen, S.H.; Boom, J.H. Trehalose-cored amphiphiles for membrane protein stabilization: importance of the detergent micelle size in GPCR stability. *Tetrahedron Letters* **1990**, *31*, 1131-1134.

29 (a) Chattopadhyay, A.; and London, E. *Anal. Biochem*., **1984**, *139*, 408–412; (b) Y. Sonoda, S. Newstead, N. J. Hu, Y. Alguel, E. Nji, K. Beis, S. Yashiro, C. Lee, J. Leung, A. D. Cameron, B. Byrne, S. Iwata and D. Drew, *Structure*, **2011**, *19*, 17–25; (c) Caffrey, M.; Li, D.; and Dukkipati, A.; *Biochemistry*, **2012**, *51*, 6266–6288. (a) Chattopadhyay, A.; and London, E. Trehalose-cored amphiphiles for membrane protein stabilization: importance of the detergent micelle size in GPCR stability. *Anal. Biochem*., **1984**, *139*, 408–412; (b) Y. Sonoda, S.; Newstead, N. J.; Hu, Y.; Alguel, E.; Nji, K.; Beis, S.; Yashiro, C.; Lee, J.; Leung, A. D.; Cameron, B.; Byrne, S.; Iwata and Drew, D.; Benchmarking membrane protein detergent stability for improving throughput of high-resolution X-ray structures. *Structure*, **2011**, *19*, 17–25; (c) Caffrey, M.; Li, D.; and Dukkipati, A. Membrane protein structure determination using crystallography and lipidic mesophases: recent advances and successes. *Biochemistry*, **2012**, *51*, 6266–6288.

30 Oliver, R. C.; Lipfert, J.; Fox, D. A.; Lo, R. H.; Doniach, S.; and Columbu, L. Dependence of micelle size and shape on detergent alkyl chain length and head group. *PLoS One*, **2013**, *8*, e62488.

31 Chae, P. S.; Gotfryd, K.; Pacyna, J.; Miercke, L. J.; Rasmussen, S. G.; Robbins, R. A.; Rana, R. R.; Loland, C. J.; Kobilka, B.; Stroud, R.; Byrne, B.; Gether, U. and Gellman, S. H., Tandem Facial Amphiphiles for Membrane Protein Stabilization. *J. Am. Chem. Soc.* **2010**, *132*, 16750-16752.

32 Deckert, G.; Warren, P. V.; Gaasterland, T.; Young, W. G.; Lenox, A. L.; Graham, D. E.; Overbeek, R.; Snead, M. A.; Keller, M.; Aujay, M.; Huber, R.; Feldman, R. A.; Short, J. M.; Olsen, G. J.; and Swanson, R. V. The complete genome of the hyperthermophilic bacterium Aquifex aeolicus. *Nature*, **1998**, *392*, 353–358.

33 Yamashita, A.; Singh, S. K.; Kawate, T.; Jin, Y.; and Gouaux, E. Crystal structure of a bacterial homologue of Na+/Cl--dependent neurotransmitter transporters. *Nature*, **2005**, *437*, 215–223.

34 Quick, M.; and Javitch, Monitoring the function of membrane transport proteins in detergent-solubilized form. J. A. *Proc. Natl. Acad. Sci. U. S. A*., **2007**, *104*, 3603–3608.

35 (a) Guan, L.; Nurva, S.; Ankeshwarapu, S. P. Mechanism of melibiose/cation symport of the melibiose permease of Salmonella typhimurium. *J. Biol. Chem*. **2011**, *286*, 6367−6374. (b) Ethayathulla, A. S.; Yousef, M. S.; Amin, A.; Leblanc, G.; Kaback, H. R.; Guan, L. Structure-based mechanism for Na+/melibiose symport by MelB. *Nat. Commun*. **2014**, *5*, 3009. (c) Amin, A.; Ethayathulla, A. S.; Guan, L. Suppression of conformation-compromised mutants of Salmonella enterica serovar Typhimurium MelB. *J. Bacteriol*. **2014**, *196*, 3134−3139. (d) Amin, A.; Hariharan, P.; Chae, P. S.; Guan, L. Effect of detergents on galactoside binding by Melibiose permeases. *Biochemistry* **2015**, *54*, 5849−5855. (e) Cordat, E.; Mus-Veteau, I.; Leblanc, G. Structural Studies of the Melibiose Permease of Escherichia coli by Fluorescence Resonance Energy Transfer II. Identification of the tryptophan residues. *J. Biol. Chem*. **1998**, *273*, 33198−33202.

36 Rosenbaum, D. M.; Cherezov, V.; Hanson, M. A.; Rasmussen, S. G.; Thian, F. S.; Kobilka, T. S.; Choi, H. J.; Yao, X. J.; Weis, W. I.; Stevens, R. C.; and Bobilka, B. K. High-resolution crystal structure of an engineered human β2-adrenergic G protein–coupled receptor. *Science*, **2007**, *318*, 1266–1273.

37 Mansoor, S. E.; McHaour H. S.; and Farrens, D. L. Mapping proximity within proteins using fluorescence spectroscopy. A study of T4 lysozyme showing that tryptophan residues quench bimane fluorescence. *Biochemistry*, **2002**, *41*, 2475–2484.

38 Yao, X.; Parnot, C.; Deupi, X.; Ratnala, V. R. P.; Swaminath, G.; and Farrens, D. Coupling ligand structure to specific conformational switches in the β **2**-adrenoceptor. *Nat. Chem. Biol*., **2006**, *2*, 417–422.

39 Swaminath, G.; Steenhuis, J.; Kobilka, B.; and Lee, T. W. Allosteric modulation of β2-adrenergic receptor by Zn2+. *Mol. Pharmacol*., **2002**, *61*, 65–72.

40 J. M., Sunahara, R. K., Pardo, L., Weis, W. I., Kobilka, B. K. and Granier, S. Crystal structure of the μ-opioid receptor bound to a morphinan antagonist. *Nature,* **2012,** *485*, 321-326

41 Ruta, V., Jiang, Y., Lee, A., Chen, J. and MacKinnon, R. Functional analysis of an archaebacterial voltage-dependent K^+ channel. *Nature* **2003**, *422*, 180–185.

42 Sadaf, A.; Jonas S. Mortensen, Capaldi, C.; Tikhonova, E.; Hariharan, P.; Ribeiro, O.; Loland, C.; Guan, L.; Byrne, B.; and Chae, P. S. A class of rigid linker-bearing glucosides for membrane protein structural study. *Chem. Sci.***, 2016**, *7***,** 1933-1939

43 Hussain, H.; Yang, D.; Tikhonova, E.; Mortensen, J. S.; Ribeiro, O.; Santillan, C.; Das, M.; Ehsan, M.; Loland, C.; Guan, L.; Kobilka, K.; Byrne, B.; Chae, P.S. Resorcinarene-based facial glycosides: implication of detergent flexibility on membrane protein stability. *Chem. Eur. J.,* **2017**, *23*, 6724-6729.